International Journal of Heat and Mass Transfer 78 (2014) 224–231

Contents lists available at ScienceDirect

International Journal of Heat and Mass Transfer

journal homepage: www.elsevier.com/locate/ijhmt

Technical Note

Pool boiling experiments in reduced graphene oxide colloids part II – Behavior after the CHF, and boiling hysteresis

Ho Seon Ahn [a], Ji Min Kim [b], Massoud Kaviany [c,d], Moo Hwan Kim [c,*,1]

[a] Division of Mechanical System Engineering, Incheon National University, Incheon, Republic of Korea
[b] Department of Mechanical Engineering, POSTECH, Pohang, Republic of Korea
[c] Division of Advanced Nuclear Engineering, POSTECH, Pohang, Republic of Korea
[d] Department of Mechanical Engineering, University of Michigan, Ann Arbor, USA

ARTICLE INFO

Article history:
Received 5 February 2013
Received in revised form 23 May 2014
Accepted 19 June 2014

Keywords:
Pool boiling
Critical heat flux
Boiling heat transfer
Graphene
Hysteresis

ABSTRACT

The critical heat flux (CHF) during reduced graphene oxide (RGO) colloid pool boiling was increased by the development of coating layers from the RGO flakes. By boiling water after boiling RGO colloid, we confirmed that the CHF enhancement was due to the development of RGO coating layers such as the base graphene layer (BGL), self-assembled foam-like graphene structure (SFG), and thickly aggregated graphene layer (TGL). During RGO colloid boiling, we observed an interesting phenomenon after the CHF point: when the heat flux reached the maximum value (CHF), the wall temperature slowly began to increase while the heat flux was maintained, unlike the rapid wall temperature increase that is observed during water boiling. We examined the stability of this phenomenon and the boiling hysteresis in relation to the heat flux. We hypothesized that the BGL and SFG could induce this phenomenon by functioning as heat spreaders, owing to the greatly enhanced thermal conductivity during the formation of hot/dry spots, and the vapor escape resistance during boiling on a porous medium.

1. Introduction

Boiling is an efficient mode of heat transfer, and is employed for this purpose in component cooling and various energy conversion systems. The quest for improved equipment performance and the demand created by new high-density energy systems continue to motivate studies on boiling heat transfer. However, boiling is an extremely complicated process, and continues to challenge inquisitive minds. The nature of the pool boiling process varies considerably, depending on the conditions under which boiling occurs. The level of heat flux, thermo-physical properties of the liquid and vapor, surface material and its finish, and physical size of the heated surface may all affect the boiling process. Fig. 1(a) illustrates the boiling regimes encountered on a horizontal flat surface as its temperature is increased. If the surface temperature of the heated material is controlled and slowly increased, the boiling curve will resemble the blue curve of Fig. 1(b). On the other hand, if the heat flux is controlled and slowly increased, the boiling curve takes on a different character, and will resemble the red curve of Fig. 1(b). One difference between temperature-controlled and heat-flux-controlled conditions is that in the latter case, when the heat flux is increased beyond the critical heat flux (CHF), the surface temperature jumps to a much higher temperature on the film boiling curve to deliver the increased heat flux. Since most thermal systems are operated under heat-flux-controlled conditions, the CHF is an important operating limit for preventing heater failure due to sharp increases in the wall temperature. Nanofluid boiling [1–11], micro/nano engineered surfaces [12–17], and capillary porous structures [18–21] not only enhance boiling heat transfer and the CHF, but may also cause various hysteresis phenomena. The numerous variations of boiling heat transfer hysteresis are more clearly manifested on surfaces with porous coatings than on smooth surfaces. Hysteresis is an important phenomenon, and should be included in the analysis of boiling heat transfer on a surface with a porous coating. Experimental boiling hysteresis curves exhibit diverse shapes, depending on the geometrical and thermal parameters of the porous coating and the physical properties of the liquid [22] (see Figs. 2 and 3).

Graphene has recently attracted considerable attention due to its high thermal conductivity (900–5000 $WK^{-1}m^{-1}$) [23]. Since graphene exists as ultra-thin and microscale flakes, a great deal of effort has been expended to synthesize large-area films that

* Corresponding author. Address: Korea Institute of Nuclear Safety, Daejeon, Republic of Korea.
E-mail address: mhkim@postech.ac.kr (M.H. Kim).
[1] This author is currently working in Korea Institute of Nuclear Safety (KINS) as a president.

http://dx.doi.org/10.1016/j.ijheatmasstransfer.2014.06.055
0017-9310/

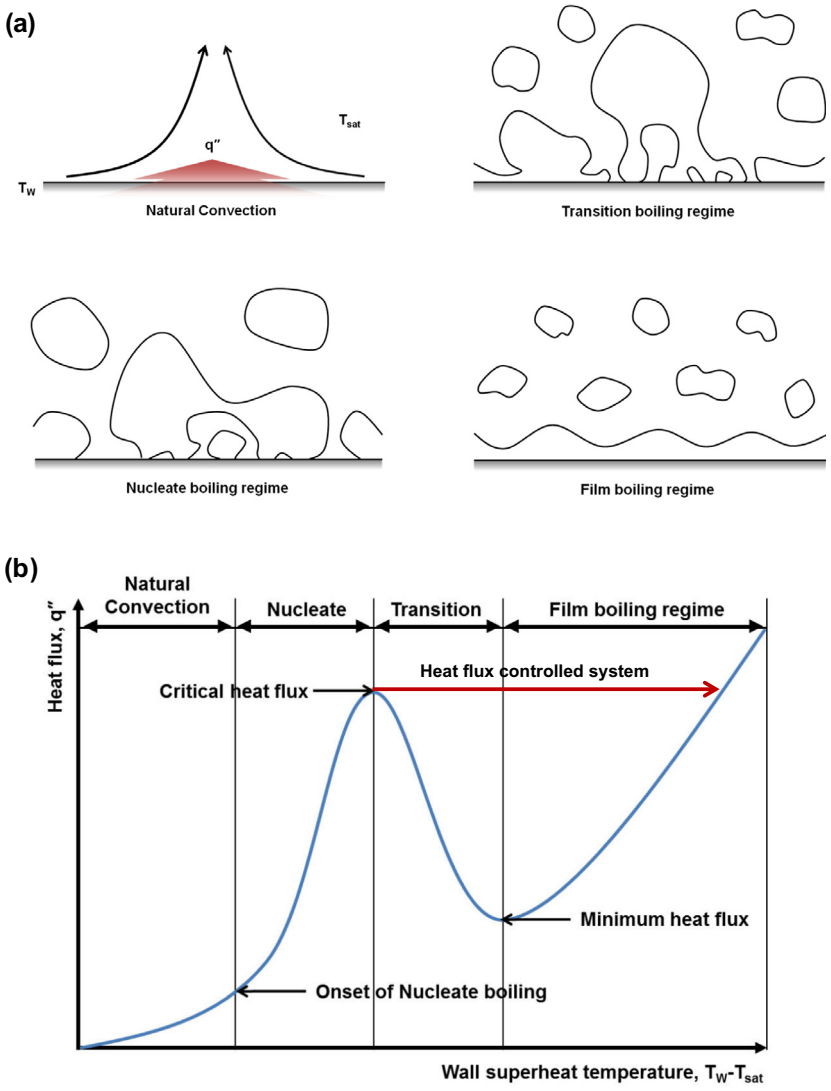

Fig. 1. (a) Boiling regimes (b) normal boiling curve.

retain its superb properties. In particular, soluble graphene in water/solvent has been synthesized via the oxidation of graphene. Through a chemical process with hydrazine, graphene oxide (GO) can be converted to a reduced graphene oxide (RGO), which can exhibit properties similar to graphene. Soluble graphene in water (RGO colloid) could be used as a working fluid for boiling heat transfer. According to a number of previous studies of nanofluid boiling [1–11], we can expect surface modifications through the deposition of RGO flakes on the heater during nucleate boiling. We assume that RGO colloid boiling is the simplest method of applying graphene to a thermal system. In Part I (boiling characteristics in RGO colloids) [24], we investigated the effects of RGO flake coatings on the onset of nucleate boiling (ONB), CHF, and boiling heat transfer (BHT) during atmospheric pool boiling, distinguishing between the base graphene layer (BGL), the self-assembled foam-like graphene structure (SFG), and the thickly aggregated graphene layer (TGL).

In this study, CHF experiments with RGO colloids were conducted in an orderly manner, to examine the effects of RGO flake coatings on the CHF enhancement. An *ad hoc* test was employed, in which water boiling was carried out after RGO flake coating. We observed interesting boiling characteristics after the CHF that have not been reported elsewhere. We also investigated boiling hysteresis during RGO colloid boiling, water boiling after RGO flake coating, and boiling after the CHF.

2. Experimental results and discussion

In Part 1, the experimental procedure, facilities, and test samples were fully described. [24] We begin by describing the RGO flake coatings deposited via nucleate boiling of RGO colloids. Depending on the colloid concentration, the RGO coatings were the BGL, SFG, and TGL, indicated by (A), (B), and (C) shaded light gray, dark gray, and black, respectively, in Fig. 4.

2.1. Ad hoc tests to examine the CHF enhancement during RGO colloid boiling

We conducted several sets of CHF tests with RGO colloid boiling under saturated condition of atmospheric pressure, using colloid concentrations of 0.0001, 0.0005, and 0.0010 wt.%. As the concentration of the RGO colloid decreased, the CHF increased. The reason for this was revealed by analyzing the RGO coating history in terms of the BGL, SFG, and TGL. Each type of coating exhibited distinctive characteristics [24]:

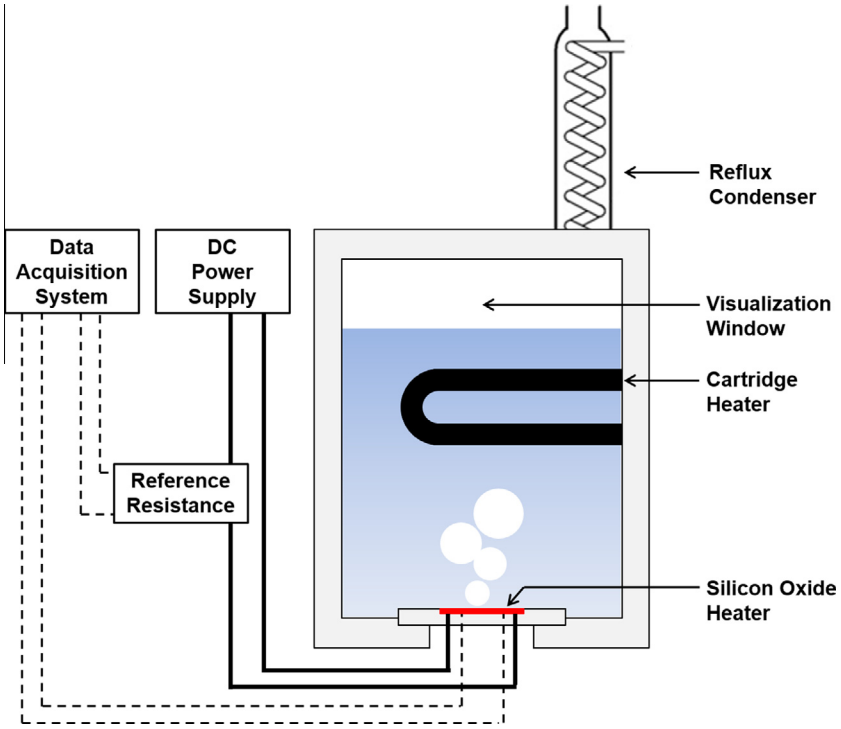

Fig. 2. The schematic diagram of the pool boiling experimental facility.

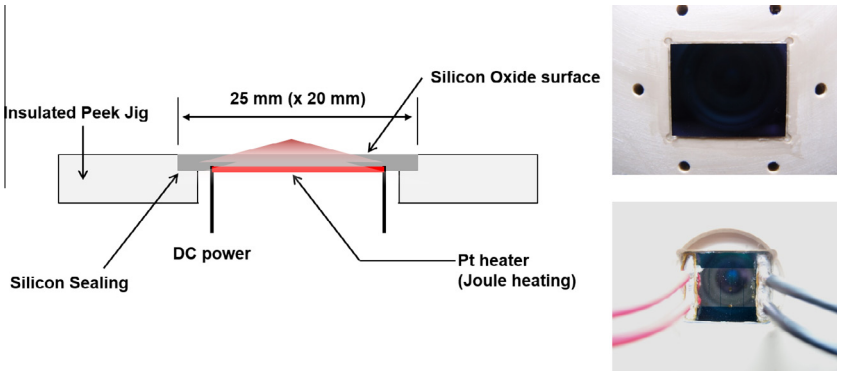

Fig. 3. Test heater (SiO_2 substrate and platinum film heater).

1. The BGL can provide enhanced thermal activity, owing to its high conductivity [25].
2. The BGL and SFG can respectively provide hydrophilic and hydrophobic wettability. However, water absorption has been observed on both them.
3. The formation of the BGL, SFG, and TGL depends on the applied heat flux and the concentration of the RGO colloid.
4. RGO coating layers such as the SFG (above the BGL) have exhibited water absorption.

These RGO coatings provided CHF enhancement in accordance with the above facts.

We employed some *ad hoc* tests to confirm the RGO coating effect on the CHF enhancement. In these tests, water boiling up to the CHF was carried out after RGO coating via colloid boiling. Fig. 5 shows the CHF enhancement results of the *ad hoc* tests. During RGO colloid boiling, the CHF increased as the concentration decreased. However, the CHF values from the water boiling tests were similar to each other, the highest being the value obtained from the test conducted after RGO coating via the 0.0001 wt.% colloid. We compared the RGO coatings before and after water boiling. Fig. 6 shows images of the test heaters after the RGO colloid and water boiling tests, indicating that nucleate boiling and thermal shock (rapid increase in the wall temperature) due to the CHF during water boiling caused the RGO coatings to detach themselves from the heater. When CHF occurs in RGO colloid boiling, the RGO coatings were fully remained, but in water boiling were partially remained as shown in Fig. 6. This means that nucleate boiling can induce both deposition and detachment of RGO flakes, the former during RGO colloid boiling and the latter during water boiling. If RGO flakes are supplied by an RGO colloid, deposition will be dominant. If not, detachment will be dominant [11]. The stacking order of the RGO coatings (BGL, SFG, and TGL) can be seen in Fig. 6, and was the same as described in Part 1 [24]. In Fig. 5, the CHF during water boiling after RGO coating was higher than the CHF during RGO colloid boiling. As the concentration increased, the difference between water and RGO colloid boiling became larger. As Fig. 6 indicates, the TGL (black color) was removed by water

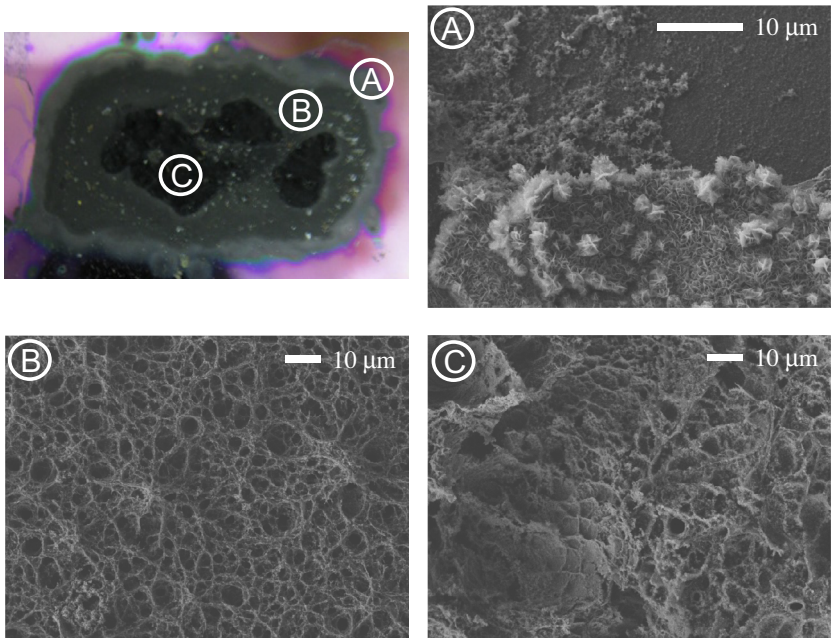

Fig. 4. After RGO colloid boiling; BGL, SFG, and TGL.

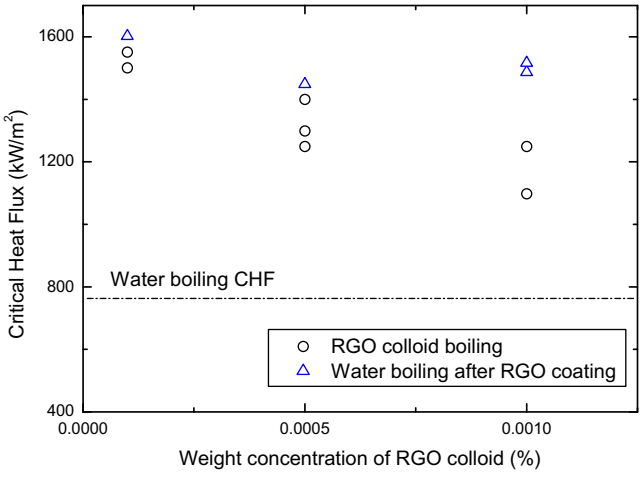

Fig. 5. CHF enhancement during RGO colloid boiling and during water boiling after RGO colloid boiling for different concentrations of RGO colloid.

boiling. Since the BGL, SFG, and TGL were stacked in that order, some portions of the BGL (light gray color) and SFG (dark gray color) remained on the heater. Nucleate boiling eliminated the TGL (which creates thermal resistance) from the stack of RGO coating layers [24]. Therefore, it can be inferred that the BGL and SFG were adequate to increase the CHF.

2.2. A transient boiling heat transfer phenomenon during RGO colloid boiling

In our previous studies, we defined the CHF as the point on the boiling curve where the wall temperature increased suddenly and rapidly under steady-state conditions [26]. In this study, however, we defined the CHF as the maximum value on the boiling curve, because a transient boiling phenomenon was observed at the maximum heat flux during RGO colloid boiling at concentrations of 0.0005 and 0.0010 wt.%, as shown in Fig. 7. During water boiling, when the heat flux reached the maximum value, the wall temperature increased rapidly (in 2 s) from 143 to 200 °C. However, during RGO colloid boiling, when the heat flux reached the maximum value (80% enhancement vs. water boiling), the wall temperature increased very slowly (over 10,200 s = 170 min) from 150 to 220 °C. The curves shown in Fig. 7 indicate the average values obtained by increasing/decreasing the heat flux step under steady-state conditions. After the CHF was reached during water boiling, the values correspond to raw data that were sampled at 1-s intervals. After the CHF was reached during RGO colloid boiling, the values correspond to time-averaged data that were calculated at 1-min intervals; these do not indicate a steady-state condition because the wall temperature increased slowly and continuously. We refer to this interesting phenomenon that occurred after the CHF as transient boiling heat transfer. Fig. 8 shows the heat flux and wall temperature trends vs. time, sampled at 1-min intervals after the heat flux reached the maximum value. The heat flux was maintained and the wall temperature increased slowly. Fig. 9 shows the heat flux and wall temperature trends vs. time and RGO colloid concentration. During 0.0001 wt.% RGO colloid boiling, we did not observe transient boiling heat transfer. As with plain water boiling, the wall temperature increased rapidly and the heat flux decreased rapidly for this case. However, RGO colloid boiling with colloid concentrations of 0.0005 and 0.0010 wt.% exhibited both the transient boiling heat transfer and CHF enhancement.

In a previous study [27], we used high-speed visualization to determine that transient boiling heat transfer could be induced by the formation of a dry patch in the mushroom bubble that forms at the maximum heat flux. The dry patch did not expand far enough to trigger the CHF, and hence the wall temperature did not increase rapidly. We hypothesized that the BGL and SFG could play two major roles in transient boiling heat transfer. First, we focused on its role as a heat spreader for the BGL and SFG during nucleate boiling. The effective thermal conductivity of dry graphene foam has been measured by Pettes et al. [28], and is much smaller than that of the dense layer formed adjacent to the surface of BGL (beneath the SFG). Based on the results of Shin and Kaviany [29], we expect the junction thermal conductivity between graphene flakes in the foam and the BGL to be controlled by forces

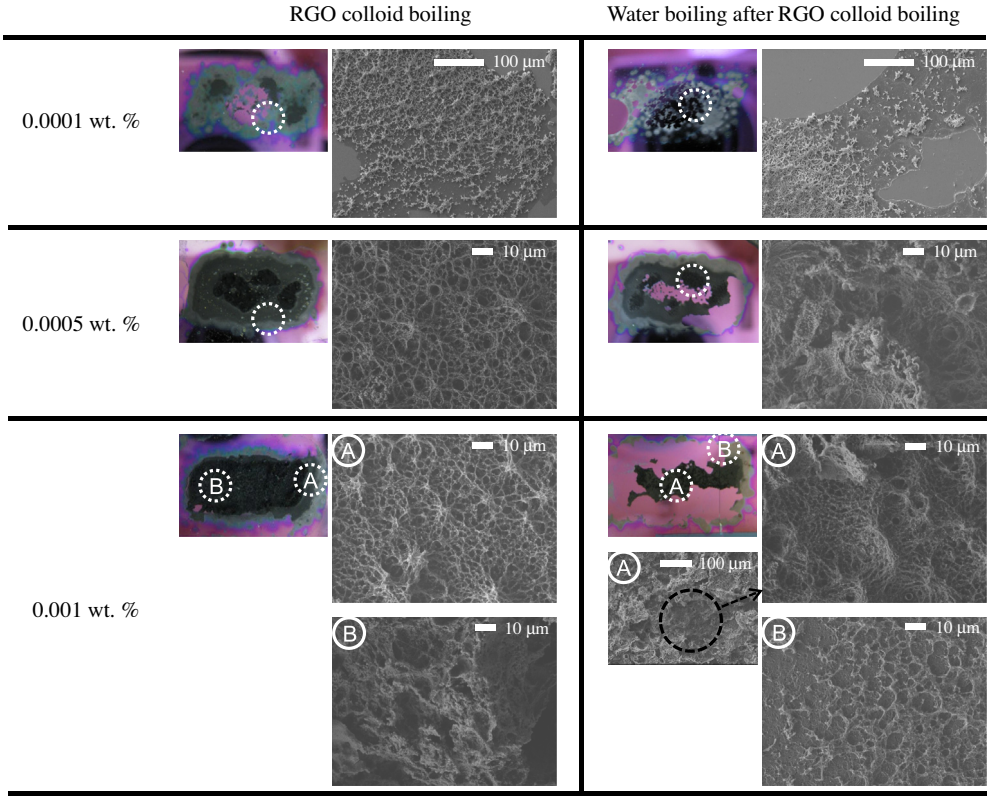

Fig. 6. Surface investigation of RGO coatings for different RGO colloid concentrations.

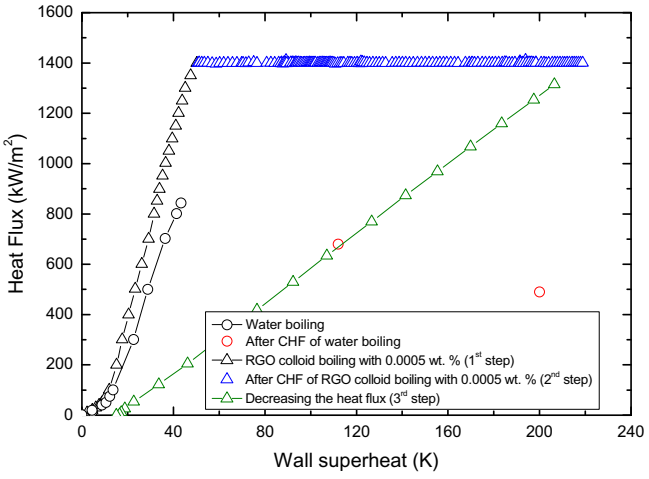

Fig. 7. Boiling curve for 0.0005 wt.% RGO colloid boiling.

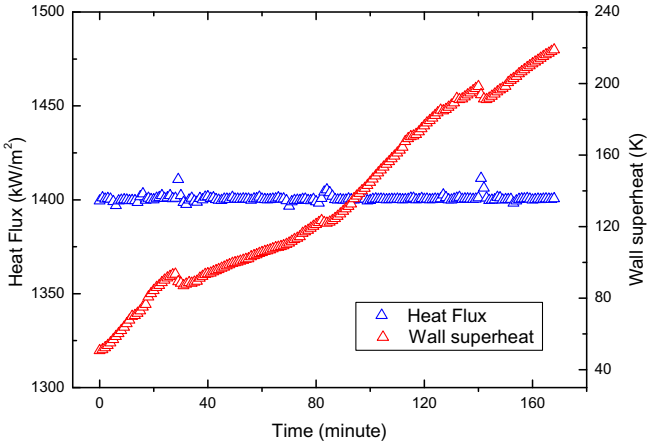

Fig. 8. Time history of the heat flux and wall superheat during transient boiling heat transfer.

stronger than the van der Waals forces (e.g., covalent bonds). Accordingly, we expect the BGL to have an effective thermal conductivity one or two orders of magnitude greater than that of the graphene foam. According to Jang et al. [25], the estimated thermal conductivity of a graphene multilayer is 110–1100 $W K^{-1} m^{-1}$, depending on its thickness. As the graphene multilayer thickened from 1 to 100 nm on the silicon substrate, the thermal conductivity increased. In the present study, the effective thermal conductivity of the BGL would be enough to exceed that of the silicon dioxide substrate by at least one order of magnitude, since the thickness of the BGL was roughly 50–100 nm. Here, we used the concept of thermal activity [30], defined as follows:

$$S = \delta\sqrt{\rho_h c_h k_h} \quad (1)$$

where S, δ, ρ_h, c_h, and k_h are the thermal activity, heater characteristic dimension, density, specific heat, and thermal conductivity of the heater material, respectively. The greatly improved thermal activity (S) of the BGL (compared to the silicon dioxide substrate) could increase the CHF by delaying hot/dry spot formation and growth [31]. Near the CHF, the depletion of liquid under the mushrooming bubbles leads to the creation of local dry spots, whose temperatures rise steeply under the influence of the imposed heat flux. The rate of temperature increase is moderated by the capacity of the underlying structure to locally absorb and/or conduct heat to parts of the heater still experiencing nucleate boiling. If the heater is very thin or has poor thermal properties, the CHF occurs soon after the formation of dry spots on the heater surface. On the other hand, if the thickness and thermal properties are more favorable, the heater

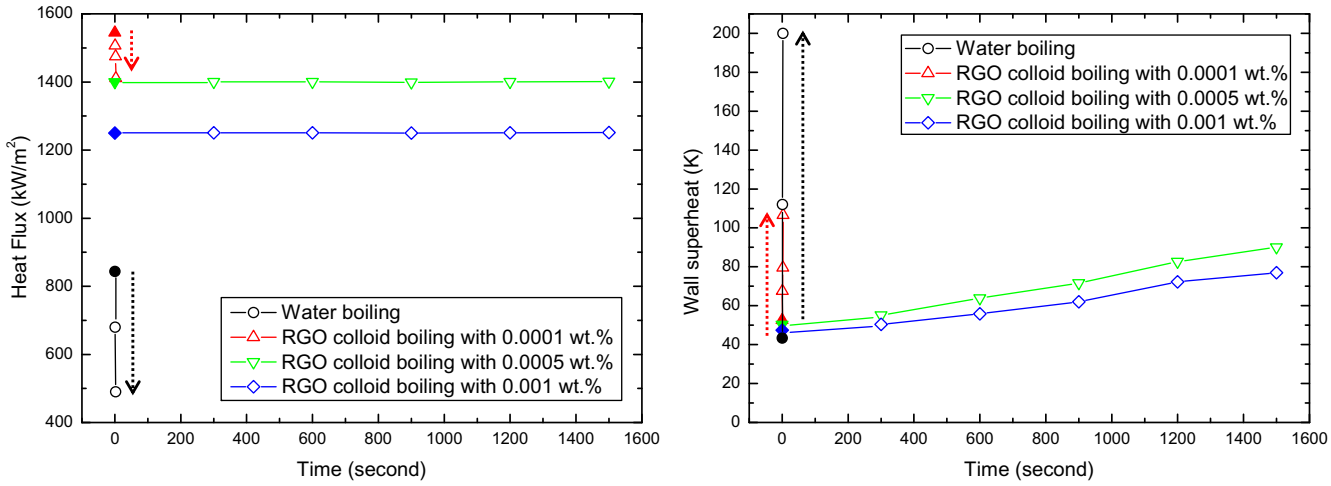

Fig. 9. Time history of the heat flux and wall superheat after the maximum heat flux for different concentrations of RGO colloid.

will successfully absorb and conduct the heat away from local dry spots, thus preventing the dry spot temperature from exceeding the critical re-wet temperature. For sufficiently high S, the heater may be able to sustain the sequential formation and extinction of many dry spots, relying on subsequent re-wetting to locally cool the surface back to the nucleate boiling regime [31]. Finally, the BGL beneath the SFG could play the role of a heat spreader, thus preventing the dry patch from expanding.

It could also be hypothesized that the SFG prevents the CHF from being triggered because it is a saturated porous medium with many micro-sized pores. Fukusako et al. [32] studied transition and film boiling on a liquid-saturated porous bed. They plotted a boiling curve without the CHF for the porous medium, where neither the wall temperature nor the heat flux could maintain a steady state, and both increased gradually. They postulated that transition boiling between nucleate and film boiling is characterized by a wetted surface and vapor film conditions. Their boiling characteristics showed a gradual increase, but differed in some respects from those of the present study (zero superheat at the ONB and low heat flux at the beginning of transition boiling). We anticipate that visualization results for transition boiling on a porous medium could provide some answers in the present study. However, the confined condition of our porous medium caused it to be liquid-saturated. In addition, Berenson [33] postulated that the roughness (peak-to-peak) of the heater surface influences transition boiling (where nucleate boiling transitions to film boiling after experiencing the CHF). The roughness makes it possible for the liquid to meet the solid, because of the unstable vapor film, so that transition boiling on the SFG can be maintained over a much longer time period, instead of rapidly transitioning to film boiling.

2.3. Boiling hysteresis

As Fig. 7 shows, we stopped our transient boiling heat transfer when the wall temperature reached 220 °C, to prevent the solder between the PT electrode and the electric lead line from melting. We decreased the heat flux to examine its relationship to boiling hysteresis in the boiling curve, and also because nucleate boiling continued during transient boiling heat transfer, and if it continued over a sufficient amount of time, the RGO coating would undergo additional significant changes. The boiling hysteresis (right-shifted boiling curve) while decreasing the heat flux was determined, as shown in Fig. 7. We compared the coatings from the 0.0005 wt.% RGO colloid boiling before and after the transient boiling heat transfer. The results are shown in Fig. 10, which clearly indicates the gray-scale levels of the RGO coatings. After 170 min of transient boiling heat transfer, there were three gray-scale levels, corresponding to the BGL, SFG, and TGL. However, before transient boiling heat transfer, there were only two gray-scale levels, corresponding to the BGL and SFG. This is clear evidence that the TGL was formed during transient boiling heat transfer. Thus, the boiling hysteresis while decreasing the heat flux was induced by the TGL, which was formed by long-term nucleate boiling during transient boiling heat transfer. Next, we examined the stability of transient boiling heat transfer with respect to the heat flux and the RGO colloid. Fig. 11 shows that the heat transfer was maintained, even though the heat flux increased. In both Regions 1 and 2, the wall temperature increased continuously and slowly. We concluded that transient boiling heat transfer could be used to maintain the heat flux and eliminate rapid increases in the wall temperature, continuing to function even when the heat flux increases.

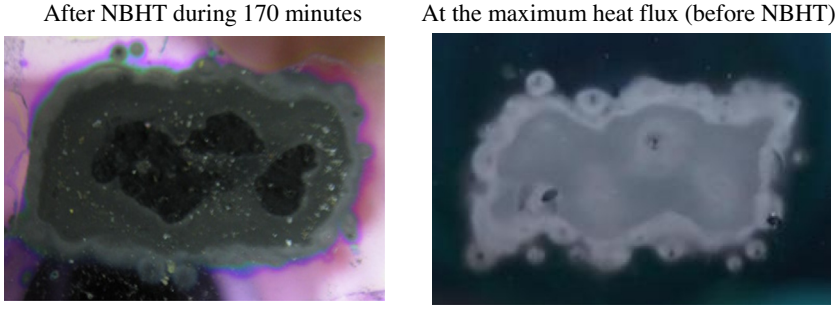

Fig. 10. Comparison of heater optical images with and without transient boiling heat transfer.

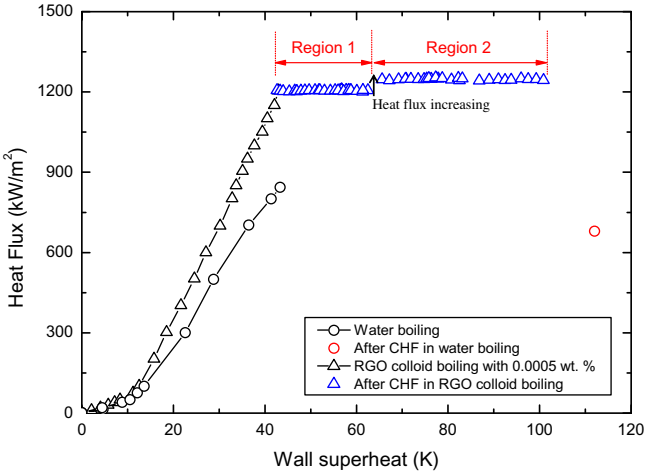

Fig. 11. Boiling curves to examine the stability of transient boiling heat transfer.

Fig. 12 shows the boiling curve for the *ad hoc* test of water boiling after boiling 0.0005 wt.% RGO colloid. In the region indicated by the blue circle, we observed boiling hysteresis (inverted, left-shifted boiling curve) under the same heat flux and wall temperature conditions for both RGO colloid boiling and water boiling (explained as an effect of boiling on a porous medium). Such a hysteresis has been observed mainly during water boiling on capillary porous surfaces with relatively high thicknesses or low structure permeability. Both high thickness and weak structure permeability are conducive to increasing the vapor and liquid flow resistance, which leads to the generation and sustaining of a vapor layer inside the pores [34–36]. According to Wojcik [37], the shape of a boiling curve with this type of hysteresis depends on remembered values of the heating surface (such as heat flux and wall temperature), and thus could be called hysteresis with memory. In the *ad hoc* test, lower performance was observed than during transient boiling heat transfer with RGO colloid. We hypothesized that the detachment of the RGO coatings during water boiling induced this lower performance. At a wall temperature of 240 °C, we decreased the heat flux, as indicated by the green curve in Fig. 12. Unlike the boiling hysteresis during RGO colloid boiling (shown in Fig. 7), the boiling characteristics were nearly recovered on the boiling curve for water. It is interesting to note that the first recovered point was close to the inverted boiling hysteresis. This means that while the heat flux was decreasing, the boiling remembered the boiling characteristics of the existing RGO coating layer.

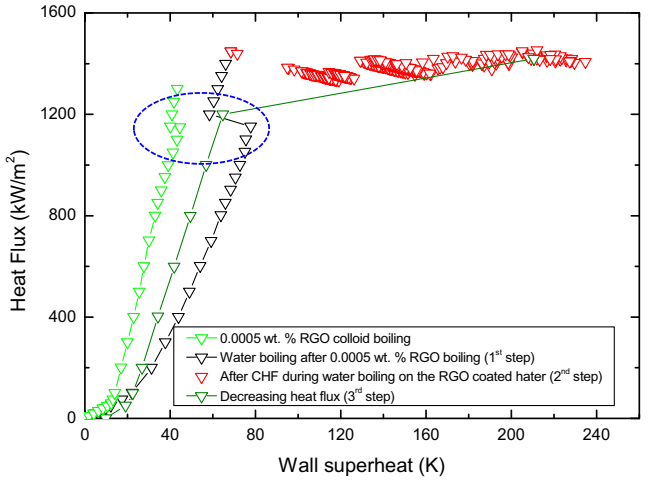

Fig. 12. Boiling curve of RGO colloid boiling and water boiling after RGO colloid boiling.

3. Conclusions

In this paper, we studied the CHF enhancement caused by boiling RGO colloid in detail. We observed an interesting transient boiling phenomenon that occurred after the CHF, and boiling hysteresis. During RGO colloid boiling, the RGO coating layers – the base graphene layer (BGL), the self-assembled foam-like graphene structure (SFG), and the thickly aggregated graphene layer (TGL) – were developed and stacked in that order, depending on the heat flux. The following are our new findings.

- We carried out *ad hoc* tests to confirm the effect of the RGO coating layers on the CHF enhancement. During water boiling, the TGL was completely detached. Portions of the BGL and SFG remained, and the CHF was increased by their heat-spreading actions, and through the effects of boiling on a porous medium, as described in our related work [24].
- We discovered a transient boiling heat transfer that occurs after the CHF during RGO colloid boiling. Even when the heat flux reached the maximum value, the wall temperature increased very slowly while the heat flux was maintained, unlike the rapid increase in wall temperature that occurs during water boiling. We hypothesize that this resulted from delayed hot/dry spot formation, due to the heat-spreading action of the BGL and SFG, and from the effects of boiling on a porous medium. During transient boiling heat transfer, the TGL was formed, and could have induced the observed boiling hysteresis. We investigated the boiling hysteresis due to the TGL formation while increasing/decreasing the heat flux.

Conflict of interests

None declared.

Acknowledgments

This work was supported by the National Research Foundation of Korea (NRF) grant funded by the Korea government (MEST) (2012R1A1A2002900).

Appendix A. Supplementary data

Supplementary data associated with this article can be found, in the online version, at http://dx.doi.org/10.1016/j.ijheatmasstransfer.2014.06.055.

References

[1] H.D. Kim, J.B. Kim, M.H. Kim, Effect of nanoparticles on CHF enhancement in pool boiling of nano-fluids, Int. J. Heat Mass Transfer 49 (25–26) (2006) 5070–5074.
[2] H.D. Kim, M.H. Kim, Experimental study of CHF characteristics of water–TiO_2 nano-fluids, Nucl. Eng. Technol. 38 (2006) 61–68.
[3] I.C. Bang, S.H. Chang, Boiling heat transfer performance and phenomena of Al_2O_3–water nano-fluids from a plain surface in a pool, Int. J. Heat Mass Transfer 48 (2005) 2407–2419.
[4] H.D. Kim, J.B. Kim, M.H. Kim, Experimental studies on CHF characteristics of nano-fluids at pool boiling, Int. J. Multiphase Flow 33 (2007) 691–706.
[5] S.J. Kim, I.C. Bang, J. Buongiorno, L.W. Hu, Effects of nanoparticle deposition on surface wettability influencing boiling heat transfer in nanofluids, Appl. Phys. Lett. 89 (15) (2006) 153107.
[6] H.D. Kim, M.H. Kim, Effect of nanoparticle deposition on capillary wicking that influences the critical heat flux in nanofluids, Appl. Phys. Lett. 91 (1) (2007) 014104.
[7] H.S. Ahn, S.H. Kang, H.J. Jo, H. Kim, M.H. Kim, Visualization study of the effects of nanoparticles surface deposition on convective flow boiling CHF from a short heated wall, Int. J. Multiphase Flow 37 (2011) 215–228.
[8] Z. Liu, L. Liao, Sorption and agglutination phenomenon of nanofluids on a plane heating surface during pool boiling, Int. J. Heat Mass Transfer 51 (2008) 2593–2601.

[9] J.S. Coursey, J. Kim, Nanofluid boiling: the effect of surface wettability, Int. J. Heat Fluid Flow 29 (2008) 1577–1585.
[10] Y.H. Jeong, W.J. Chang, S.H. Chang, Wettability of heated surfaces under pool boiling using surfactant solutions and nano-fluids, Int. J. Heat Mass Transfer 51 (2008) 3025–3031.
[11] S.M. Kwark, R. Kumar, G. Moreno, J. Yoo, S.M. You, Pool boiling characteristics of low concentration nanofluids, Int. J. Heat Mass Transfer 53 (5–6) (2010) 972–981.
[12] H.S. Ahn, H.J. Jo, S.H. Kang, M.H. Kim, Effect of liquid spreading due to nano/microstructures on the critical heat flux during pool boiling, Appl. Phys. Lett. 98 (2011) 071908.
[13] H.S. Ahn, C. Lee, J. Kim, M.H. Kim, The effect of capillary wicking action of micro/nano structures on pool boiling critical heat flux, Int. J. Heat Mass Transfer 55 (2012) 89–92.
[14] K.-H. Chu, R. Enright, E.N. Wang, Structured surfaces for enhanced pool boiling heat transfer, Appl. Phys. Lett. 100 (2012) 241603.
[15] V. Khanikar, I. Mudawar, T. Fisher, Effects of carbon nanotube coating on flow boiling in a micro-channel, Int. J. Heat Mass Transfer 52 (2009) 3805–3817.
[16] R. Chen, M.-C. Lu, V. Srinivassn, Z. Wang, H.H. Cho, A. Majumdar, Nanowires for enhanced boiling heat transfer, Nano Lett. 9 (2009) 548–553.
[17] M.-C. Lu, R. Chen, V. Srinivasan, V.P. Carey, A. Majumdar, Critical heat flux of pool boiling on Si nanowire array-coated surfaces, Int. J. Heat Mass Transfer 54 (2011) 5359–5367.
[18] C.Y. Wang, P. Cheng, Multiphase flow and heat transfer in porous media, Adv. Heat Transfer 30 (1997) 93–196.
[19] S.G. Liter, M. Kaviany, Pool-boiling CHF enhancement by modulated porous-layer coating: theory and experiment, Int. J. Heat Mass Transfer 44 (2001) 4287–4311.
[20] Y. Tang, B. Tand, Q. Li, J. Qing, L. Lu, K. Chen, Pool-boiling enhancement by novel metallic nanoporous surface, Exp. Therm. Fluid Sci. 44 (2013) 194–198.
[21] B.J. Zhang, K.J. Kim, H. Yoon, Enhanced heat transfer performance of alumina sponge-like nano-porous structures through surface wettability control in nucleate pool boiling, Int. J. Heat Mass Transfer 55 (2012) 7487–7498.
[22] M.E. Poniewski, Peculiarities of boiling heat transfer on capillary-porous coverings, Int. J. Therm. Sci. 43 (2004) 431–442.
[23] A.A. Balandin, S. Ghosh, W. Bao, I. Calizo, D. Teweldebrhan, F. Miao, C.N. Lau, Superior thermal conductivity of single-layer graphene, Nano Lett. 8 (3) (2008) 902–907.
[24] H.S. Ahn, J.M. Kim, M. Kaviany, M.H. Kim, Pool boiling experiments of reduced graphene oxide colloid: part I – boiling characteristics, Int. J. Heat Mass Transfer 74 (2014) 501–512.
[25] W. Jang, Z. Chen, W. Bao, C.N. Lau, C. Dames, Thickness-dependent thermal conductivity of encased graphene and ultrathin graphite, Nano Lett. 10 (10) (2010) 3909–3913.
[26] H.S. Ahn, M.H. Kim, Visualization study of critical heat flux mechanism on a small and horizontal copper heater, Int. J. Multiphase Flow 41 (2012) 1–12.
[27] H.S. Ahn, J.M. Kim, C. Park, J.-W. Jang, J.S. Lee, H. Kim, M. Kaviany, M.H. Kim, A novel role of three dimensional graphene foam to prevent heater failure during boiling, Sci. Rep. 3 (1960) (2013) 1–2.
[28] M.T. Pettes, H. Ji, R.S. Ruoff, L. Shi, Thermal transport in three-dimensional foam architectures of few-layer graphene and ultrathin graphite, Nano Lett. 12 (2012) 2959–2964.
[29] S. Shin, M. Kaviany, Interflake thermal conductance of edge-passivated graphene, Phys. Rev. B 84 (2011) 235433.
[30] M. Arik, A. Bar-Cohen, Effusivity-based correlation of surface property effects in pool boiling CHF of dielectric liquid, Int. J. Heat Mass Transfer 46 (2003) 3755–3765.
[31] M. Arik, A. Bar-Cohen, S.M. You, Enhancement of pool boiling critical heat flux in dielectric liquid by microporous coating, Int. J. Heat Mass Transfer 50 (2007) 997–1009.
[32] S. Fukusako, T. Komoriya, N. Seki, An experimental study of transition and film boiling heat transfer in liquid-saturated porous bed, ASME J. Heat Transfer 108 (1986) 117–124.
[33] P.J. Berenson, Experiments on pool-boiling heat transfer, Int. J. Heat Mass Transfer 5 (1962) 985–999.
[34] A.E. Bergles, M.C. Chyu, Characteristics of nucleate pool boiling from porous metallic coatings, ASME J. Heat Transfer 104 (1982) 279–285.
[35] J.Y. Chang, S.M. You, Boiling heat transfer phenomena from micro-porous and porous surfaces in saturated FC-72, Int. J. Heat Mass Transfer 40 (1997) 4437–4447.
[36] N.H. Afgan, L.A. Jovic, S.A. Kovalev, V.A. Lenykov, Boiling heat transfer from surfaces with porous layers, Int. J. Heat Mass Transfer 28 (1985) 415–422.
[37] T.M. Wojcik, Experimental investigations of boiling heat transfer hysteresis on sintered, metal-fibrous, porous structures, Exp. Therm. Fluid Sci. 33 (2009) 397–404.